Biochemical and Biophysical Research Communications 457 (2015) 183–186

Contents lists available at ScienceDirect

Biochemical and Biophysical Research Communications

journal homepage: www.elsevier.com/locate/ybbrc

Use of 1–4 interaction scaling factors to control the conformational equilibrium between α-helix and β-strand

Yuan-Ping Pang *

Computer-Aided Molecular Design Laboratory, Mayo Clinic, Rochester, MN 55905, USA

ARTICLE INFO

Article history:
Received 11 December 2014
Available online 25 December 2014

Keywords:
Secondary structure elements
α-Helix
β-Strand
Protein backbone torsions
1–4 Nonbonded interaction scaling factors
Force field

ABSTRACT

1–4 interaction scaling factors are used in AMBER forcefields to reduce the exaggeration of short-range repulsion caused by the 6–12 Lennard-Jones potential and a nonpolarizable charge model and to obtain better agreements of small-molecule conformational energies with experimental data. However, the effects of these scaling factors on protein secondary structure conformations have not been investigated until now. This article reports the finding that the 1–4 interactions among the protein backbone atoms separated by three consecutive covalent bonds are more repulsive in the α-helix conformation than in two β-strand conformations. Therefore, the 1–4 interaction scaling factors of protein backbone torsions ϕ and ψ control the conformational equilibrium between α-helix and β-strand. Molecular dynamics simulations confirm that reducing the ϕ and ψ scaling factors readily converts the α-helix conformation of AcO-$(AAQAA)_3$-NH_2 to a β-strand conformation, and the reverse occurs when these scaling factors are increased. These results suggest that the ϕ and ψ scaling factors can be used to generate the α-helix or β-strand conformation *in situ* and to control the propensities of a forcefield for adopting secondary structure elements.

1. Introduction

The additive AMBER forcefield is an empirical potential energy function in the form of Eq. (1) with a set of parameters to describe the relationship between a molecular structure and its energy [1–9]. In Eq. (1), the A_{ij} and B_{ij} constants for the atoms separated by three consecutive covalent bonds are divided by a 1–4 van der Waals interaction scaling factor (SCNB) to reduce the exaggeration of short-range repulsion caused by the 6–12 Lennard-Jones potential and a nonpolarizable charge model [3]; the C constant for the atoms separated by three consecutive covalent bonds is also divided by a 1–4 electrostatic interaction scaling factor (SCEE) for better agreements of small-molecule conformational energies with experimental data [3]. While the effects of these 1–4 interaction scaling factors on structure and energy of small molecules and carbohydrates are known in the literature [1–3,10], the effects of SCNB and SCEE on protein secondary structure conformations have not been clear until now.

$$E = \Sigma k_b(b-b_0)^2 + \Sigma k_\theta(\theta-\theta_0)^2 + \Sigma k_\phi[\cos(n\phi+\delta)+1] + \Sigma(A_{ij}r_{ij}^{-12} - B_{ij}r_{ij}^{-6} + Cq_iq_jr_{ij}^{-1}) \quad (1)$$

This article reports the finding that the 1–4 interactions among the protein backbone atoms separated by three consecutive covalent bonds are more repulsive in the α-helix conformation than in two β-strand conformations. Therefore, the 1–4 interaction scaling factors for protein backbone torsions ϕ and ψ control the conformational equilibrium between α-helix and β-strand in molecular dynamics simulations. Using model peptide AcO-$(AAQAA)_3$-NH_2, a pentadecapeptide known to adopt the α-helix conformation in water [11] and abbreviated as AAQAA hereafter, molecular dynamics simulations show (1) that reducing the ϕ and ψ scaling factors readily converts the α-helix conformation of AAQAA to β-strand conformations, and (2) that increasing these scaling factors converts the anti-parallel β-strand conformation of AAQAA to the α-helix conformation. The results suggest that these scaling factors can be used in practical applications to regulate the conformational equilibrium between α-helix and β-strand.

2. Methods

2.1. Low-mass molecular dynamics simulations

In this study low-mass molecular dynamics (LMD) simulations with particle masses systemically reduced by tenfold were

Abbreviations: AcO-$(AAQAA)_3$-NH_2, AAQAA; ALN, the Ala residue amidated by NH_2; LMD, low-mass molecular dynamics; CαβRMSD, Cα and Cβ root mean square deviation; SCNB, 1–4 van der Waals interaction scaling factor; SCEE, 1–4 electrostatic interaction scaling factor.

* Address: Stabile 12-26, Mayo Clinic, 200 First Street SW, Rochester, MN 55905, USA.

E-mail address: pang@mayo.edu

http://dx.doi.org/10.1016/j.bbrc.2014.12.084
0006-291X/

performed for enhanced configurational sampling [12]. AAQAA in the α-helix or anti-parallel β-strand conformation was solvated with 1028 or 1619 TIP3P water molecules [13], respectively, to keep the closest distance between any atom of AAQAA and the edge of the periodic solvent box at 8.2 Å using LEAP of AmberTools 1.5 (University of California, San Francisco). The anti-parallel β-strand conformation of was generated by MacPyMOL Version 1.5.0 (Schrödinger LLC, Portland, OR). The α-helix conformation was obtained from an LMD simulation that converted the anti-parallel β-strand conformation to the α-helix conformation. As provided in Dataset S1, the forcefield parameters for the Ala residue amidated by NH_2 (ALN) were generated according to a published procedure using both α-helix and β-strand conformations for the RESP charge calculation [3,14]. The solvated AAQAA was then energy-minimized for 100 cycles of steepest-descent minimization followed by 900 cycles of conjugate-gradient minimization to remove close van der Waals contacts using SANDER of AMBER 11 (University of California, San Francisco), heated from 0 to 300 K at a rate of 10 K/ps under constant temperature and volume, and finally simulated in 20 unique and independent LMD simulations using PMEMD of AMBER 11 with a periodic boundary condition at a constant temperature of 300 K and a constant pressure of 1 atm with isotropic molecule-based scaling. The 20 unique seed numbers for initial velocities of Simulations 1–20 are 1804289383, 846930886, 1681692777, 1714636915, 1957747793, 424238335, 719885386, 1649760492, 596516649, 1189641421, 1025202362, 1350490027, 783368690, 1102520059, 2044897763, 1967513926, 1365180540, 1540383426, 304089172, and 1303455736, respectively. All these isothermal–isobaric LMD simulations used (1) a dielectric constant of 1.0, (2) the Berendsen coupling algorithm [15], (3) the Particle Mesh Ewald method to calculate long-range electrostatic interactions [16], (4) a time step of 1.0 fs, (5) SHAKE-bond-length constraints applied to all the bonds involving the H atom, (6) a protocol to save the image closest to the middle of the "primary box" to the restart and trajectory files, (7) a formatted restart file, (8) atomic masses that are systemically reduced by ten-fold, (9) zeroed torsion potentials for ϕ, ψ, ϕ', and ψ', (10) 1.0 for SCNBs of ϕ and ψ and SCEEs of ϕ and ψ or 2.0 for SCNBs of ϕ and ψ and SCEEs of ϕ and ψ, and (11) default values of all other inputs of PMEMD. Each simulation was performed on a 12-core Apple Mac Pro with Intel Westmere (2.40/2.93 GHz).

2.2. Secondary structure content analysis

Using PTRAJ of AmberTools 1.5 (University of California, San Francisco), torsions ϕ and ψ of each residue in AAQAA were computed from 2000 (or 4000) conformations saved at 100-ps intervals of a 0.2-μs (or 0.4-μs) isothermal–isobaric LMD simulation of AAQAA, respectively, with simulation conditions described above. Residue X was considered to be in the α-helical conformation if all torsions ψ and ϕ of Residues X, $^{\pm1}$N, $^{\pm2}$N, and $^{\pm3}$N were within the ψ range (−67° to −27°) and the ϕ range (−77° to −37°), respectively. Residue X was in the β-strand conformation if all torsions ψ and ϕ of Residues X and $^{\pm1}$N were within the ψ range (−159° to −99°) and the ϕ range (93°–155°), respectively. Residues $^{\pm1}$N, $^{\pm2}$N, and $^{\pm3}$N are six nearby residues of Residue X (*viz.*, X–^{1}N–^{2}N–^{3}N, $^{-1}$N–X–^{1}N–^{2}N, $^{-2}$N–$^{-1}$N–X–^{1}N, and $^{-3}$N–$^{-2}$N–$^{-1}$N–X for the helix; X–^{1}N and $^{-1}$N–X for the strand). The torsion ranges are based on the reported torsions [17] for the right-handed 3.6_{13}-helix (ϕ of −57° and ψ of −47°), anti-parallel β-strand (ϕ of −139° and ψ of 135°), and parallel β-strand (ϕ of −119° and ψ of 113°) plus or minus 20°. A component α-helix or β-strand population for each residue in AAQAA was defined as the number of the α-helix or β-strand conformation of the residue divided by the number of all conformations of AAQAA saved at 100-ps intervals. Averaging the α-helix or β-strand component populations of residues 1–15 gave rise to the corresponding population for AAQAA of one LMD simulation. Averaging the α-helix or β-strand populations of a set of 20 unique and independent LMD simulations gave rise to the aggregated α-helix or β-strand population for AAQAA for the set. The standard deviation of the aggregated α-helix or β-strand population was calculated according to Eq. (2), wherein N is the number of all simulations, P_i is the α-helix or β-strand population of the ith simulation, and $\bar{P}$ is the aggregated α-helix or β-strand population. The experimental α-helix population of AAQAA in water at 300 K was obtained from averaging component helicities that were calculated according to Eqs. (1) and (2) of Ref. [11] with T_m and ΔT values and their standard deviations taken from Table 1 of Ref. [11].

$$\text{Standard Deviation} = \sqrt{\Sigma(P_i - \bar{P})^2/(N-1)} \quad (2)$$

3. Results and discussion

3.1. Repulsions among protein backbone atoms in the α-helix or β-strand conformation

Using dialanine as a model peptide (Fig. 1), this author finds that distances ^{1}C–^{2}C and ^{1}N–^{2}N in the α-helical conformation are 16–23% shorter than those in the anti-parallel and parallel β-strand conformations of the peptide (Table 1), wherein ^{X}C and ^{X}N are the carbonyl carbon atom and the amide nitrogen atom of Residue X, respectively. With the exception of the ^{1}N–^{2}N distance in the anti-parallel β-strand conformation, the ^{1}C–^{2}C and ^{1}N–^{2}N distances are shorter than the sums of the corresponding van der Waal's radii regardless of the secondary structure conformations (Table 1). In addition, the partial atomic charges of the carbonyl carbon atom and the amide nitrogen atom of one residue are identical to those of other residues as defined in additive AMBER forcefields. The 1–4 interactions between ^{1}C and ^{2}C and between ^{1}N and ^{2}N are more repulsive in the α-helix conformation than in two β-strand conformations. Therefore, it is conceivable that the 1–4 interactions between ^{1}C and ^{2}C and between ^{1}N and ^{2}N of any amino acid sequence are more repulsive in the α-helix conformation than in the β-strand conformations.

3.2. Interconversion between α-helix and β-strand conformations of AAQAA

Because protein backbone torsions ϕ and ψ govern the ^{1}C–^{2}C and ^{1}N–^{2}N distances, respectively, the afore-described finding suggests that increasing SCNBs of ϕ and ψ and/or SCEEs of ϕ and ψ can lessen the repulsions among 1–4 backbone atoms more in the α-helical conformation than in the two β-strand conformations and can consequently increase the propensity of a forcefield for the α-helical conformation and decrease the propensity for the two β-strand conformations. To test this hypothesis, a set of 20 unique, independent, all-atom, isothermal–isobaric, and 400-ns LMD simulations of AAQAA in the anti-parallel conformation were carried out at 300 K and 1 atm using the FF14SB forcefield (AMBER 14 reference manual, 29–31) with 2.0 set for SCNBs of ϕ and ψ and SCEEs of ϕ and ψ. For comparison, another set of 20 unique, independent, all-atom, isothermal–isobaric, and 200-ns LMD simulations were performed under the same simulation conditions, except that the SCNBs and SCEEs were all reduced to 1.0. In both sets of simulations, all four backbone torsion potentials (ϕ, ψ, ϕ' and ψ') of the FF14SB forcefield were zeroed to remove influences of these torsions on the effects of the SCNBs and SCEEs on the secondary structure conformations.

When using 2.0 for the SCNBs and the SCEEs, the initial anti-parallel β-strand conformation of AAQAA completely converted, within 10 ns, to the α-helix and other non-β-strand conformations

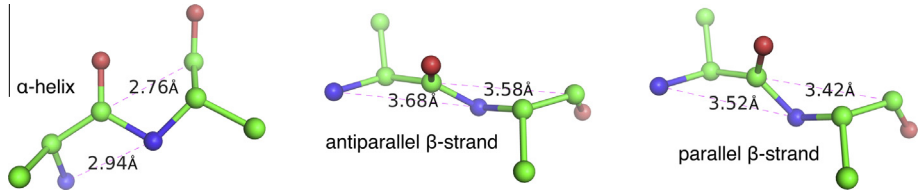

Fig. 1. The repulsive distances between 1–4 backbone atoms of dialanine in different secondary structure conformations.

Table 1
Distances between backbone atoms of dialanine and their corresponding sums of van der Waals radii.

Conformation	^{1}C–^{2}C		^{1}N–^{2}N		$R_{1C}^{*} + R_{2C}^{*}$ (Å)	$R_{1N}^{*} + R_{2N}^{*}$ (Å)
	(Å)	Δ (%)	(Å)	Δ (%)		
α-Helix	2.76	–	2.94	–	3.816	3.648
Anti-parallel β-strand	3.58	23	3.68	20	3.816	3.648
Parallel β-strand	3.42	19	3.52	16	3.816	3.648

^{X}C and ^{X}N are the carbonyl carbon atom and the amide nitrogen atom, respectively, in residue X of the dialanine, respectively. $\Delta = (\text{distance}_{\text{strand}} - \text{distance}_{\text{helix}})/\text{distance}_{\text{strand}}$.

in all 20 simulations. This is evident from the observation that the aggregated α-helix and β-strand populations of AAQAA with standard deviations of the 20 simulations at the 10-ns instant are 30 ± 18% and 0 ± 0%, respectively (Table S1). The aggregated α-helix population with its standard deviation of the 20 simulations increased to 61 ± 27% at the 400-ns instant, whereas the aggregated β-strand population remained at zero (Table 2). Visual inspection revealed that the initial anti-parallel β-strand conformation converted to a full α-helix conformation with hydrogen bonds involving the AcO and NH_2 protecting groups in 14 out of the 20 400-ns simulations (Fig. 2). As indicated by the relatively large standard deviation, the aggregated α-helix population is not fully converged at the aggregated timescale of 8 μs. Nevertheless, the aggregated β-strand population is converged, and the aggregated α-helix population of 61 ± 27% is already higher than the experimental α-helix population of 20.8 ± 0.4% for AAQAA in water at 300 K according to nuclear magnetic resonance spectroscopic data [11] (see Section 2.2). These results indicate that the modified FF14SB forcefield with 2.0 for the SCNBs and the SCEEs has a high propensity for the α-helix conformation and a low propensity for the β-strand conformation.

By contrast, when using 1.0 for the SCNBs and the SCEEs, none of the 20 200-ns simulations showed conversion from the initial anti-parallel β-strand conformation to the α-helix conformation. The aggregated α-helix and β-strand populations with standard deviations of the 20 200-ns simulations are 0 ± 0% and 25 ± 3%, respectively (Table 2). The small standard deviations indicate that these aggregated α-helix and β-strand populations are converged at the aggregated timescale of 4 μs. Visual inspection revealed various β-hairpin conformations that are in frequent exchange with extended β-strand conformations (Fig. 2). Formations of these β-hairpins require different AAQAA residues to adopt the loop conformation, which explains why the aggregated β-strand population is lower than the aggregated α-helix population. These results show that the modified FF14SB forcefield with 1.0 for the SCNBs and the SCEEs has a low propensity for the α-helix conformation and a high propensity for the β-strand conformation.

The two sets of simulations described above were then repeated with a full α-helix conformation as the initial AAQAA conformation. This conformation was identified from the afore-described simulations using 2.0 for the SCNBs and the SCEEs and the anti-parallel β-strand conformation as the initial conformation. When using 2.0 for the SCNBs and the SCEEs, no conversion from the α-helix conformation to the β-conformation was found in any of the 20 400-ns simulations. The aggregated α-helix and β-strand populations with standard deviations of the 20 400-ns simulations are 89 ± 1% and 0 ± 0%, respectively (Table 2). As indicated by the small standard deviations, both the α-helix and β-strand populations are converged at the aggregated timescale of 8 μs. These results confirm that the modified FF14SB forcefield with 2.0 for the SCNBs and the SCEEs has a high propensity for adopting the α-helix conformation and a low propensity for the β-strand conformation. When using 1.0 for the SCNBs and the SCEEs, the initial full α-helix conformation completely converted, within 10 ns, to β-strand conformations in all 20 200-ns LMD simulations (Table S1). The aggregated α-helix and β-strand populations with standard deviations of the 20 simulations are converged to 0 ± 0% and 24 ± 1%, respectively (Table 2), which also confirms that that the modified FF14SB with 1.0 for the SCNBs and the SCEEs has a low propensity for the α-helix conformation and a high propensity for the β-strand conformation.

3.3. SCNB and SCEE as regulators for equilibrium between α-helix and β-strand

The above results show that increasing or decreasing SCNBs of ϕ and ψ or SCEEs of ϕ and ψ can raise or lower, respectively, the ratio of the α-helical conformation over the β-strand conformation in LMD simulations. This finding has practical use in peptide or protein simulations. For example, for computational studies of B-cell lymphoma 2 family proteins or proteins with latent tetratrico peptide repeat [18–20], there is often a need to perform LMD simulations to intentionally convert a fragment of a protein to the α-helical conformation in the specific environment of the fragment. This type of secondary conformation can now be generated *in situ* by performing LMD simulations of the protein with a set of new atom types for torsions ϕ and ψ of the fragment with 2.0 or 1.0 for the SCNBs and the SCEEs depending upon whether the desired conformation is α-helix or β-strand, respectively.

Table 2
The α-helix and β-strand populations of AAQAA in 20 isothermal–isobaric low-mass molecular dynamics simulations with the TIP3P water at 300 K and 1 atm.

Initial conformation	Aggregated time (μs)	SCNBs of ϕ and ψ	SCEEs of ϕ and ψ	α-Helix population ± standard deviation (%)	β-Strand population ± standard deviation (%)
β-Strand*	20 × 0.4	2.0	2.0	61 ± 27	0
β-Strand*	20 × 0.2	1.0	1.0	0	25 ± 3
α-Helix	20 × 0.4	2.0	2.0	89 ± 1	0
α-Helix	20 × 0.2	1.0	1.0	0	24 ± 1

* Anti-parallel β-strand.

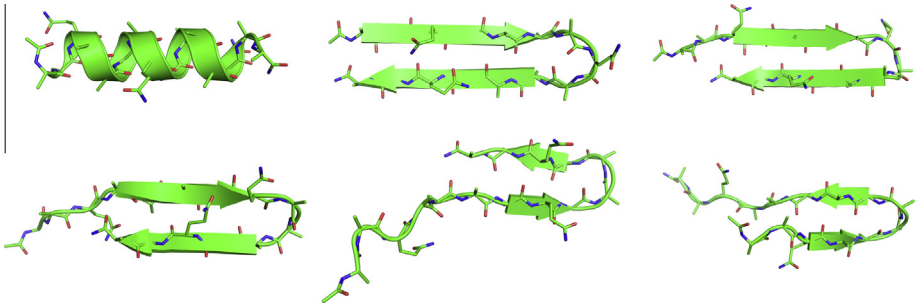

Fig. 2. AAQAA conformations identified from LMD simulations using different SCNBs and SCEEs. The α-helix conformation was identified from LMD simulations using 2.0 for SCNBs of ϕ *and* ψ and SCEEs of ϕ and ψ. The β-strand conformations were identified from LMD simulations using 1.0 for SCNBs of ϕ and ψ and SCEEs of ϕ and ψ.

In addition, the present finding also suggests that the imbalanced propensities of a forcefield for different secondary structure elements can be resolved at the root level by adjusting SCNBs of ϕ and ψ and/or SCEEs of ϕ and ψ without implementing four backbone torsions (ϕ, ψ, ϕ', and ψ') as these backbone torsions do not have physical justification [3]. For example, AMBER forcefields FF94 and FF99 are biased to the α-helix conformation [21,22], whereas FF96 has a bias to the β-strand conformation [23–26]. Adjusting SCNBs and SCEEs of the backbone torsions might balance the propensities of these AMBER forcefields without implementing ϕ, ψ, ϕ', and ψ'. A study to identify a set of the SCNBs and the SCEEs that can balance the propensities of FF99 for different secondary structure conformations is underway and will be reported in due course.

Conflict of interest

The author declares no conflict of interest.

Transparency Document

The Transparency document associated with this article can be found in the online version.

Acknowledgments

Yuan-Ping Pang acknowledges the support of this work from the US Defense Advanced Research Projects Agency (DAAD19-01-1-0322), the US Army Medical Research Material Command (W81XWH-04-2-0001), the US Army Research Office (DAAD19-03-1-0318 and W911 NF-09-1-0095), the US Department of Defense High Performance Computing Modernization Office, and the Mayo Foundation for Medical Education and Research. The contents of this article are the sole responsibility of the author and do not necessarily represent the official views of the funders.

Appendix A. Supplementary data

Supplementary data associated with this article can be found, in the online version, at http://dx.doi.org/10.1016/j.bbrc.2014.12.084.

References

[1] S.J. Weiner, P.A. Kollman, D.A. Case, U.C. Singh, C. Ghio, G. Alagona, S. Profeta, P. Weiner, A new force field for molecular mechanical simulation of nucleic acids and proteins, J. Am. Chem. Soc. 106 (1984) 765–784.
[2] S.J. Weiner, P.A. Kollman, D.T. Nguyen, D.A. Case, An all atom force field for simulations of proteins and nucleic acids, J. Comput. Chem. 7 (1986) 230–252.
[3] W.D. Cornell, P. Cieplak, C.I. Bayly, I.R. Gould, K.M. Merz Jr., D.M. Ferguson, D.C. Spellmeyer, T. Fox, J.W. Caldwell, P.A. Kollman, A second generation force field for the simulation of proteins, nucleic acids, and organic molecules, J. Am. Chem. Soc. 117 (1995) 5179–5197.
[4] P.A. Kollman, Advances and continuing challenges in achieving realistic and predictive simulations of the properties of organic and biological molecules, Acc. Chem. Res. 29 (1996) 461–469.
[5] J.M. Wang, P. Cieplak, P.A. Kollman, How well does a restrained electrostatic potential (RESP) model perform in calculating conformational energies of organic and biological molecules?, J Comput. Chem. 21 (2000) 1049–1074.
[6] Y. Duan, C. Wu, S. Chowdhury, M.C. Lee, G.M. Xiong, W. Zhang, R. Yang, P. Cieplak, R. Luo, T. Lee, J. Caldwell, J.M. Wang, P. Kollman, A point-charge force field for molecular mechanics simulations of proteins based on condensed-phase quantum mechanical calculations, J. Comput. Chem. 24 (2003) 1999–2012.
[7] J. Wang, R.M. Wolf, J.W. Caldwell, P.A. Kollman, D.A. Case, Development and testing of a general AMBER force field, J. Comput. Chem. 25 (2004) 1157–1174.
[8] V. Hornak, R. Abel, A. Okur, B. Strockbine, A. Roitberg, C. Simmerling, Comparison of multiple AMBER force fields and development of improved protein backbone parameters, Proteins 65 (2006) 712–725.
[9] K. Lindorff-Larsen, S. Piana, K. Palmo, P. Maragakis, J.L. Klepeis, R.O. Dror, D.E. Shaw, Improved side-chain torsion potentials for the AMBER ff99SB protein force field, Proteins 78 (2010) 1950–1958.
[10] K.N. Kirschner, A.B. Yongye, S.M. Tschampel, J. Gonzalez-Outeirino, C.R. Daniels, B.L. Foley, R.J. Woods, GLYCAM06: a generalizable biomolecular force field. Carbohydrates, J. Comput. Chem. 29 (2008) 622–655.
[11] W. Shalongo, L. Dugad, E. Stellwagen, Distribution of helicity within the model peptide acetyl $(AAQAA)_3$ amide, J. Am. Chem. Soc. 116 (1994) 8288–8293.
[12] Y.-P. Pang, Low-mass molecular dynamics simulation: a simple and generic technique to enhance configurational sampling, Biochem. Biophys. Res. Commun. 452 (2014) 588–592.
[13] W.L. Jorgensen, J. Chandreskhar, J.D. Madura, R.W. Impey, M.L. Klein, Comparison of simple potential functions for simulating liquid water, J. Chem. Phys. 79 (1983) 926–935.
[14] P. Cieplak, W.D. Cornell, C. Bayly, P.A. Kollman, Application of the multimolecule and multiconformational RESP methodology to biopolymers: charge derivation for DNA, RNA, and proteins, J. Comput. Chem. 16 (1995) 1357–1377.
[15] H.J.C. Berendsen, J.P.M. Postma, W.F. van Gunsteren, A. Di Nola, J.R. Haak, Molecular dynamics with coupling to an external bath, J. Chem. Phys. 81 (1984) 3684–3690.
[16] T.A. Darden, D.M. York, L.G. Pedersen, Particle mesh Ewald: an N log(N) method for Ewald sums in large systems, J. Chem. Phys. 98 (1993) 10089–10092.
[17] T.E. Creighton, Proteins, second ed., W. H. Freeman and Company, New York, 1993.
[18] Y.-P. Pang, H. Dai, A. Smith, X.W. Meng, P.A. Schneider, S.H. Kaufmann, Bak conformational changes induced by ligand binding: insight into BH3 domain binding and Bak homo-oligomerization, Sci. Rep. 2 (2012) 257.
[19] A.M. Sainski, H. Dai, S. Natesampillai, Y.-P. Pang, G.D. Bren, N.W. Cummins, C. Correia, X.W. Meng, M. Ramirez-Alvarado, D.J. Katzmann, C. Ochsenbauer, J.C. Kappes, S.H. Kaufmann, A.D. Badley, Casp8p41 generated by HIV protease kills CD4 T cells through direct Bak activation, J. Cell Biol. 206 (2014) 867–876.
[20] J.R. Lamb, S. Tugendreich, P. Hieter, Tetratrico peptide repeat interactions – to TPR or not to TPR, Trends Biochem. Sci. 20 (1995) 257–259.
[21] A.E. Garcia, K.Y. Sanbonmatsu, Alpha-helical stabilization by side chain shielding of backbone hydrogen bonds, Proc. Natl. Acad. Sci. U.S.A. 99 (2002) 2782–2787.
[22] A. Okur, B. Strockbine, V. Hornak, C. Simmerling, Using PC clusters to evaluate the transferability of molecular mechanics force fields for proteins, J. Comput. Chem. 24 (2003) 21–31.
[23] L. Wang, Y. Duan, R. Shortle, B. Imperiali, P.A. Kollman, Study of the stability and unfolding mechanism of BBA1 by molecular dynamics simulations at different temperatures, Protein Sci. 8 (1999) 1292–1304.
[24] S. Ono, N. Nakajima, J. Higo, H. Nakamura, Peptide free-energy profile is strongly dependent on the force field: comparison of C96 and AMBER95, J. Comput. Chem. 21 (2000) 748–762.
[25] J. Higo, N. Ito, M. Kuroda, S. Ono, N. Nakajima, H. Nakamura, Energy landscape of a peptide consisting of α-helix, 3(10)-helix, β-turn, β-hairpin, and other disordered conformations, Protein Sci. 10 (2001) 1160–1171.
[26] N. Kamiya, J. Higo, H. Nakamura, Conformational transition states of a β-hairpin peptide between the ordered and disordered conformations in explicit water, Protein Sci. 11 (2002) 2297–2307.